JOURNAL OF GEOPHYSICAL RESEARCH, VOL. 99, NO. C5, PAGES 10,121–10,129, MAY 15, 1994

# Mechanism for low-frequency variability and salt flux in the Mediterranean salt tongue

Michael A. Spall[1]

Woods Hole Oceanographic Institution, Woods Hole, Massachusetts

**Abstract.** The role of baroclinic instability in the generation of low-frequency variability in the interior of ocean subtropical gyres and its possible importance in the zonal flux of salt and heat within the Mediterranean salt tongue are discussed. The observed zonal enhancement of the low-frequency variability is interpreted as the signature of baroclinic instability of the large-scale wind-driven flow. The zonal orientation results from the relatively weak vertical shear of the large-scale upper ocean flow and the stabilizing influence of the planetary vorticity gradient. There is a reversal in the vertical shear of velocity at middepths in the eastern basin of the North Atlantic that results in a local middepth maximum in the zonal eddy flux of density. Linear theory predicts a vertical structure of this density flux that is nearly coincident with the observed vertical distribution of the warm, salty water of the Mediterranean salt tongue. A primitive equation model is used to investigate the nonlinear, large-amplitude regime. The zonal eddy density (or salt) flux averaged over several wavelengths and several cycles of wave growth and breaking indicates that this mechanism may be an important component in the overall salt balance in this region.

## 1. Introduction

One of the most dominant characteristics of the large-scale North Atlantic hydrography is the Mediterranean salt tongue. This feature is a warm, salty water mass centered at a depth of approximately 1100 m that extends from the Mediterranean outflow most of the way across the North Atlantic basin. Although the tongue appears as a smooth, large-scale feature in the climatological data sets, recent observations indicate that it is actually highly variable with a mixture of strong mesoscale eddies, submesoscale lenses of Mediterranean water (Meddies), and jets superimposed on the large-scale flow. Dynamical models of the salt tongue have traditionally interpreted the large-scale salinity field as the steady balance between advection by the large-scale flow and diffusion supplied by mixing due to unresolved mesoscale eddies and vertical processes [e.g. *Richardson and Mooney,* 1975; *Hogg,* 1987]. The actual mechanisms by which the time-dependent flow transports salt within the Mediterranean tongue, and their relationship to the large-scale hydrography, are not well understood.

Recent observations indicate the presence of low-frequency zonal motions within the core of the salt tongue. *Müller and Siedler* [1992] find zonal variability with periods of 3–4 years in a 9-year current meter record located at 33°N, 22°W. *Spall et al.* [1993] also find zonal jet features in SOFAR float trajectories within the core of the tongue whose low-frequency eddy kinetic energy is zonally enhanced (5.7 $cm^2\ s^{-2}$ versus 2.4 $cm^2\ s^{-2}$). The zonal motions were both down the mean large-scale salinity gradient (to the west) and up the large-scale salinity gradient (to the east). *Schmitz et al.* [1988] note a similar zonal enhancement both within the Mediterranean salt tongue and elsewhere within the subtropical gyre of the North Atlantic.

The present study proposes baroclinic instability of the large-scale flow as a mechanism for the generation of low-frequency, primarily zonal, motion at midlatitudes. Furthermore, it is suggested that the eddy fluxes associated with this instability mechanism may make an important contribution to the westward flux of salt within the Mediterranean salt tongue. Basic ideas of the instability mechanism are developed in section 2 using linear quasi-geostrophic theory, and a primitive equation model is used to extend these results into the large-amplitude, nonlinear regime in section 3. These results are related to observations and more complex models in section 4, and final conclusions are presented in section 5.

## 2. A Baroclinic Instability Mechanism: Linear Theory

Linear theory is used to characterize the structure of the small-amplitude behavior and to gain an under-

[1] Also formerly on leave at Institut für Meereskunde, Kiel, Germany.



Paper number 93JC03587.
0148-0227/94/93JC-03587$05.00

standing of what drives the instability and how it depends on the flow parameters. The basic understanding derived from this simple analysis will aid in the interpretation of the nonlinear model results in the next section.

### 2.1. Problem Formulation

The standard linear stability equations are derived from the conservation of quasi-geostrophic potential vorticity,

$$\left[\frac{\partial}{\partial t} + J(\psi, \cdot)\right]\left[\nabla^2\psi + \beta y + \left(\frac{f_0^2}{N^2}\psi_z\right)_z\right] = 0, \quad (1)$$

where $\psi$ is the quasi-geostrophic streamfunction, the Jacobian operator is defined as $J(a,b) = a_x b_y - a_y b_x$, $f_0$ is the Coriolis parameter at the central latitude, $\beta$ is the meridional gradient of the Coriolis parameter, and $N^2$ is the Brünt Väisälä frequency.

We are interested in how small perturbations on a mean flow evolve in this system. Those perturbations which grow in time can be expected to dominate the variability, at least until finite amplitude effects become important. To derive the stability equations, it is first assumed that the streamfunction may be split into a steady two-dimensional mean state $\Psi(y,z)$ and a time-dependent perturbation $\phi(x,y,z,t)$, where $\phi \ll \Psi$ [*Pedlosky,* 1964]. This simplified decomposition is appropriate for a mean flow that is in the zonal direction only; however, we are interested in the more general case where the mean flow is directed at some angle relative to zonal. The baroclinic instability of nonzonal flows is simply related to the baroclinic instability of purely zonal flows using the following coordinate transformation [*Pedlosky,* 1979]:

$$\beta' = \beta\cos\theta \qquad U'(z) = U(z)\cos(\alpha - \theta) \quad (2)$$

The direction of the mean flow relative to east is $\alpha$, the direction of the perturbation wave vector relative to east is $\theta$, and $U(z)$ is the mean velocity. For the present analysis it is assumed that the mean flow is a function of depth only, $U(z) = -\Psi_y(z)$. For mean flows that rotate with depth, a similar transformation applies with $\alpha = \alpha(z)$. This simplification is justified here, however, as it will be shown that the results are only weakly dependent on the mean flow direction for values representative of midlatitude subtropical gyres. The following discussion refers to $U'(z)$ and $\beta'$, in the rotated coordinate frame, although the primes will be dropped for convenience.

It is further assumed that the perturbations are wavelike in nature in both the zonal and meridional directions and have a vertical structure $F(z)$.

$$\phi(x,y,z,t) = F(z)\ \exp[i(kx + ly - \omega t)] \quad (3)$$

Substitution of (3) into (1) yields an eigenvalue problem for the complex frequency $\omega = \omega_r + i\omega_i$.

$$\omega[-(k^2+l^2)F + (f_0^2/N^2F_z)_z] =$$
$$[\beta + (f_0^2/N^2\,U_z)_z]kF - [(k^2+l^2)F - (f_0^2/N^2\,F_z)_z]Uk \quad (4)$$

Positive values of the imaginary component will result in unstable modes that grow exponentially in time. The vertical boundary conditions at the top and bottom are taken to be homogeneous, that is, flat bottom with no surface forcing. It is reasonable to neglect the bottom topography because the horizontal velocity at the bottom is very weak (see Figure 1). The boundary conditions for the perturbation streamfunction are periodic in both the zonal and meridional directions, appropriate for the large-scale flow within the subtropical gyre.

The mean velocity profile and the mean stratification are required to complete the stability analysis. These background states are chosen to be representative of the real ocean, yet controlled by a very few parameters so that the basic dependence of the instability mechanism on the mean state can be most easily revealed. The mean velocity profile used in the stability analysis is based on the calculations reported by *Saunders* [1982]. Vertical profiles of the average meridional geostrophic velocity based on hydrographic data in the eastern basin (east of the mid-Atlantic ridge) are shown in Figure 1. The large-scale flow represented by these sections was believed to be primarily wind driven, hence the absolute velocity was chosen such that the net meridional transport satisfied the Sverdrup relation. The present

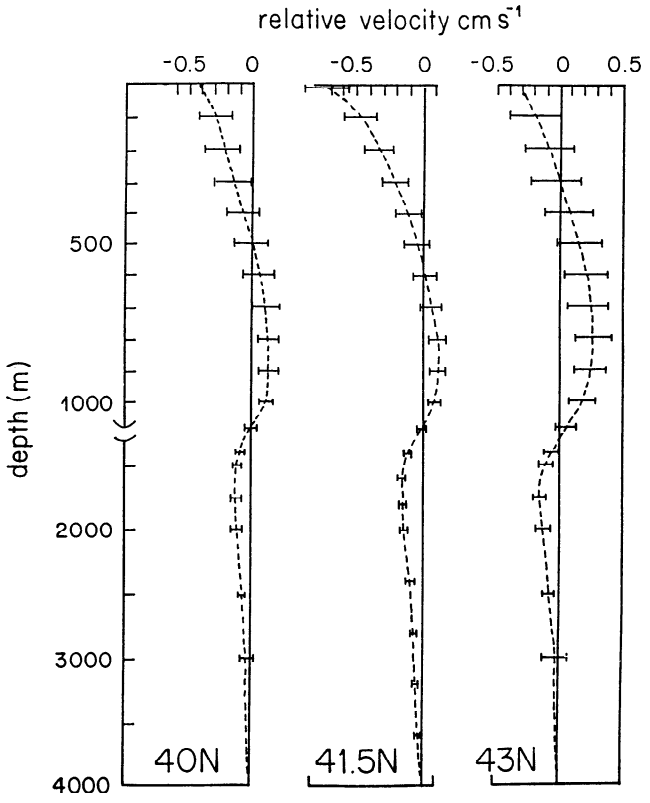


**Figure 1.** Zonally averaged meridional geostrophic velocity east of the Mid-Atlantic Ridge with error bars (redrafted from *Saunders* [1982, Figure 4]).

analysis is not overly sensitive to this choice of reference level because it is the vertical shear of the velocity that is most important for the instability mechanism. Other profiles in this region show a similar shape with weak southward flow in the upper 500 m, a reversal with northward flow between approximately 500 and 1200 m, and very weak southward flow in the deep ocean. The maximum northward velocity is at a depth near 900 m, and the secondary southward maximum is between 1500 and 2000 m depth. The climatological atlas of *Maillard* [1986] also indicates broad northward flow between 600 and 1200 m (relative to 3000 m) east of the mid-Atlantic ridge and north of 35°N. Several mechanisms have been proposed to explain this northward middepth flow, including Ekman suction in the subpolar gyre [*Schopp and Arhan,* 1986], buoyancy fluxes consistent with salt fingering within the Mediterranean salt tongue [*Arhan,* 1987], and cross-isopycnal mixing in the salt tongue [*Tziperman,* 1987].

An approximation to the profile of *Saunders* [1982] is given by the analytic expression below.

$$U(z) = U_0 e^{z/h_0} \cos\left(2\pi \frac{z}{h_0}\right) \qquad z < h_0$$

$$U(z) = 0.3678\, U_0 \left[\frac{H - z}{H - h_0}\right] \cos\left(\frac{\pi}{2}\frac{(z - h_0)}{(H - h_0)}\right) \qquad z > h_0 \tag{5}$$

The bottom depth $H = 4000$ m, $h_0 = 1800$ m represents both the depth of the second southward maximum in the velocity profile and the $e$-folding scale of the velocity in the upper thermocline, and $U_0 = -0.5$ cm s$^{-1}$ is the surface velocity. A local flow maximum is located at a depth of $h_0/2 = 900$ m. This profile qualitatively reproduces the essential features of the profiles calculated by *Saunders* [1982] (the vertical distribution is indicated in Figure 3). The mean stratification is taken to decrease exponentially with depth with a surface maximum of $4 \times 10^{-5}$ s$^{-2}$ and an $e$-folding scale of 600 m. Changes in the maximum stratification do not change the qualitative behavior of the instability; they only result in a shift in wavenumber space. The rotation parameters are taken to be representative of conditions at midlatitudes, $f_0 = 1.0 \times 10^{-4}$ s$^{-1}$ and $\beta = 2.0 \times 10^{-11}$ m$^{-1}$s$^{-1}$.

## 2.2. Horizontal Scales and Orientation

In this section the horizontal scales, orientation, and frequency of the unstable modes of the system are described. In order to demonstrate the influence of mean flow direction on the instability mechanism, we make the simplifying assumption that the only aspect of the mean flow that changes with latitude is its direction. While this is reasonable for the wind-driven component in the upper ocean, it is not a very good approximation for the middepth northward flow, which is believed to be present only north of approximately 35°N. However, the results in this section are not significantly influenced by the details of the vertical profile or the presence of the middepth northward flow. They are controlled by the relatively weak vertical shear in the upper ocean that is typical of midlatitude subtropical gyres in general and not specific to the region of the Mediterranean salt tongue. The importance of the middepth structure will be discussed in the following sections.

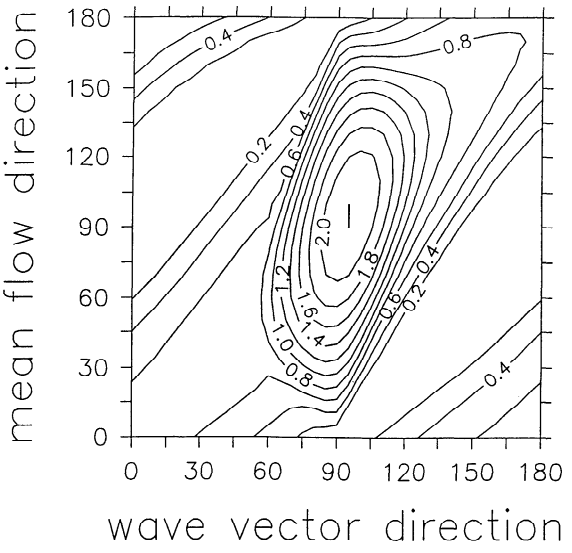


**Figure 2.** Growth rate of the fastest growing wave (years$^{-1}$) as a function of the mean flow angle ($\alpha$) and the wave vector direction ($\theta$).

The maximum growth rate as a function of the mean flow direction and perturbation wave vector direction is shown in Figure 2. For all mean flow directions between 20° and 160° the direction of propagation of the fastest growing instabilities is close to 90°, or in a nearly north–south direction. Because the horizontal velocity of the unstable waves is oriented perpendicular to the wave vector, this indicates that the fastest growing perturbations are nearly zonal for almost all mean flow angles. This preferentially zonal orientation results from the competition between maximal energy release for a wave vector oriented parallel to the mean flow and the beta effect, which stabilizes the flow for perturbations across the mean potential vorticity gradient [*Pedlosky,* 1979].

This result demonstrates that for weak vertical shears typical of subtropical gyre interiors the stabilizing influence of beta is sufficiently strong that the only perturbations that can efficiently extract energy from the mean flow are nearly zonal. For weaker vertical shears the most unstable waves are oriented even closer to 90° over the entire range of mean flow directions. Increasing the vertical shear increases the potential energy of the mean flow, thus reducing the influence of beta, and gives rise to waves which propagate more parallel to the mean flow.

At very low mean flow angles ($\alpha < 20°$, $\alpha > 160°$) the fastest growing waves are oriented nearly along the direction of the mean flow and the perturbations are

nearly perpendicular to the mean flow. For these cases, zonal perturbations are not able to tap the potential energy of the mean flow efficiently because the perturbations are nearly parallel to the mean density contours. The necessary conditions for baroclinic instability are still met when the flow is purely zonal due to the weak stratification at middepths.

The fastest growing instabilities have meridional wavelengths between 75 and 150 km. For all waves that have sigificant growth rates the absolute value of the phase speed is less than 0.1 $cm^2\ s^{-1}$, resulting in periods between 3 and 10 years. These periods are much greater than the timescale of exponential growth, thus the waves are essentially stationary during the growth of the perturbations.

### 2.3. Vertical Structure and Eddy Density Flux

In the previous section it was found that the characteristics of the unstable modes are not overly sensitive to variations in the mean flow direction between 60° and 120°. For the remainder of the paper we will assume that the mean flow is in the north–south direction only in order to investigate the possible role of the eddy density flux associated with the baroclinic instability mechanism in the zonal flux of salt.

The perturbation streamfunction for the fastest growing mode at 100 km wavelength is shown in Figure 3a. The mean velocity profile is indicated on the right as a function of depth. The characteristic tilt of the perturbation streamfunction into the mean flow is evident both in the upper ocean and at middepths, suggesting that a release of potential energy is occurring at both depths. The relatively large perturbation amplitude at middepths is a result of the velocity shear reversal and the relatively weaker stratification at this depth compared to that at the surface. In the absence of the middepth northward flow (typical of subtropical gyre interiors away from the core of the salt tongue), or for uniform vertical stratification, the vertical structure of the waves is surface intensified, consistent with the zonal jet observed in the current meter data of *Schmitz et al.* [1988] at 32°N.

The perturbation density flux ($u\rho'$) for the fastest growing mode at 100 km wavelength is shown in Figure 3b. There is clearly a net negative flux over the wavelength of the wave in the upper 800 m and a net positive flux between 800 and 1750 m. The negative flux indicates that the unstable waves are gaining energy from the mean flow in the upper thermocline through baroclinic instability. The positive flux at middepths is also indicative of energy conversion because the vertical gradient of the mean flow changes sign and, through the thermal wind relation, the horizontal density gradient also changes sign. The middepth flux is centered close to the depth of the maximum salinity anomaly in the Mediterranean salt tongue and has a similar vertical scale of 1000 m.

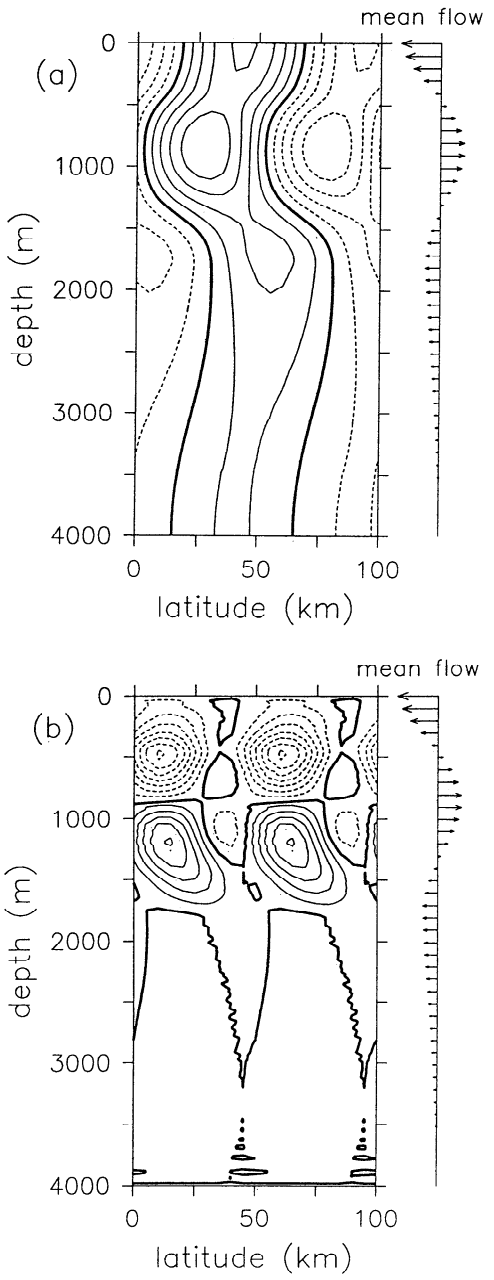


**Figure 3.** Vertical structure of the linearly most unstable mode with the mean flow indicated on the right (units arbitrary): (a) perturbation streamfunction and (b) perturbation density flux ($u'\rho'$).

The depths of the maximum and minimum perturbation density fluxes occur where $(u\rho')_z$ vanishes. For constant $N^2$ this occurs at the depth where the meridional potential vorticity gradient is zero. In the more general case of variable $N^2$ it can be shown that the maximum and minimum eddy density fluxes occur at a depth between the zero crossing of the meridional potential vorticity gradient and the steering level (depth at which $U = \omega_r k$). For the present profile this constraint requires that the minimum flux be between 400 and 450 m and that the maximum flux be between 1260 and 1350 m, in close agreement with Figure 3b.

## 3. Finite Amplitude Behavior

Although linear theory is quite useful for understanding the basic instability mechanism, it can only predict the structure and sign of the perturbation and is formally valid only for the initial growth period of the wave. Nonetheless, we are still interested in several aspects of the finite amplitude behavior of this system. For example, at finite amplitude, are the perturbations similar in magnitude and character to what has been observed in the SOFAR float and current meter data? What limits the growth of the perturbations? Is the instability mechanism influenced by the presence of mesoscale eddies superimposed on the mean flow? Can the rectified eddy fluxes account for an appreciable amount of the salt flux in the Mediterranean salt tongue?

### 3.1. The Nonlinear Model

These questions will be addressed using the nonlinear primitive equation model described by *Haidvogel et al.* [1991]. The model variables are horizontal velocity, vertical velocity, and temperature and salinity (or density). The model domain is a channel of 300 km meridional extent and 400 km longitudinal extent. The boundary conditions are periodic in north–south and free slip in east–west. The channel length is approximately 4 times the wavelength of the fastest growing waves, allowing for the development and interaction of a wide range of spatial scales. This domain is intended to represent a portion of the eastern basin between 35°N and 45°N, away from strong fronts and shallow coastal regions. The horizontal resolution is 6.25 km and the vertical profile is represented by 30 Chebychev polynomials. The deformation radius is approximately 26 km at 40°N so that it is well resolved at this horizontal resolution. The subgridscale parameterization is biharmonic in the horizontal and second order in the vertical. The coefficients of horizontal and vertical diffusion and viscosity are $1\times10^{9}$ m$^4$ s$^{-1}$ and $1\times10^{-4}$ m$^2$ s$^{-1}$, respectively. The Coriolis parameter $f = 1 \times 10^{-4}$ s$^{-1}$ and is constant to allow for periodic boundary conditions in the meridional direction. This is appropriate for an approximately north-south flow because the preferred orientation of the perturbation velocities is zonal. Its neglect may become important to the long time evolution of the zonal perturbations due to its stabilizing influence on zonal flows. However, a simple scale analysis indicates that the zonal jets that develop still satisfy the necessary conditions for baroclinic and barotropic instability even in the presence of beta.

The model is initialized with the analytic velocity profile given by (5). The fit parameters were chosen as $h_0 = 1800$ m, $U_0 = 1$ cm$^2$ s$^{-1}$, $N_0^2 = 4 \times 10^{-5}$ s$^{-2}$, and $z_0 = 600$ m. A random superposition of small perturbations between 50 and 300 km wavelength were added to the uniform velocity profile at the center of the channel, and the model was integrated for 700 days. This calculation used density only; results from similar calculations with temperature and salinity are presented in the next section.

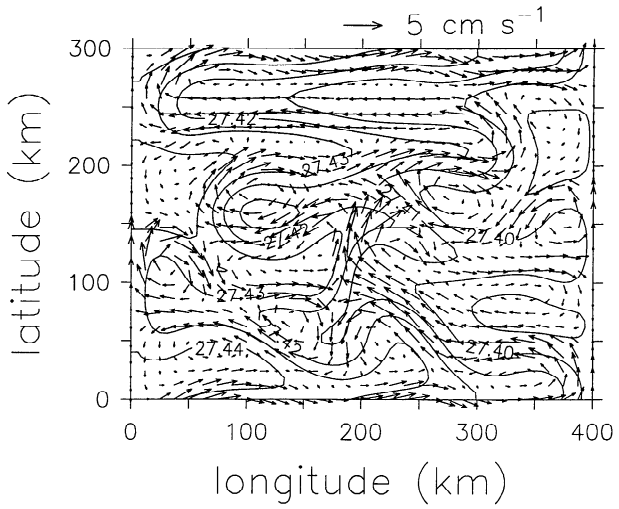


**Figure 4.** Primitive equation horizontal velocity field on day 400 at 1187 m (every other point is plotted) superimposed on the density field.

Figure 4 shows the velocity field superimposed on the density field at 1187 m on day 400. Over the first 400 days the initially meridional flow has developed elongated zonal jets which have begun to become unstable and break down into mesoscale eddies. The horizontal velocities are much larger than the mean flow, of the order of 1–5 cm s$^{-1}$ and primarily, although not exclusively, oriented in the zonal direction. This amplitude is consistent with the observed eddy kinetic energy at this depth in the Mediterranean salt tongue [*Müller and Siedler,* 1992; *Spall et al.,* 1993]. A variety of scales grow out of the initial random perturbations, however, the dominant meridional wavelengths are of the order of 100 km, in general agreement with the fastest growing instabilities based on linear theory.

The zonal density flux ($u\rho'$) on day 400 at the center of the channel is shown in Figure 5a. The basic vertical structure predicted by the simple linear theory carries over into the large-amplitude, interactive wave regime. There are negative density fluxes centered near 500 m and positive fluxes near 1200 m associated with each of the unstable waves. The meridionally averaged zonal density flux ($\overline{u\rho'}^{y}$) is shown as a function of depth and time in Figure 5b. Because the initial perturbations along the jet were very small, the density flux is small during the early (linear) stages of the calculation. The strongest perturbation density fluxes occur in the nonlinear regime, between days 250 and 700. During this time, many zonal jets develop to large amplitude and break down into mesoscale eddies, as indicated in Figure 4 for day 400. In fact, there is a significant transfer of energy from the low-frequency, zonal regime of the growing waves into the more isotropic higher-frequency

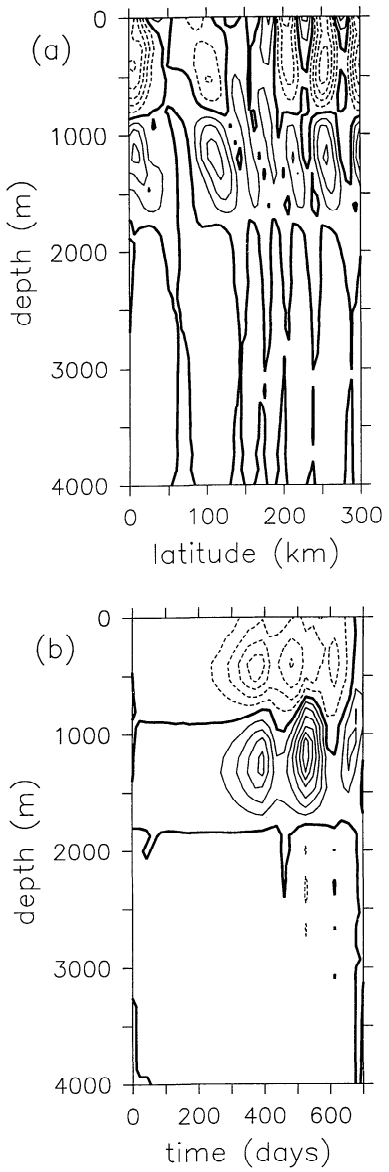


**Figure 5.** Eddy density flux ($u\rho'$) in the primitive equation calculation at the center of the channel (longitude = 200 km) (units of $10^{-6}$ g cm$^{-2}$ s$^{-1}$): (a) meridional section on day 400 (contour interval = 10) and (b) meridional average as a function of time (contour interval = 3).

mesoscale band as a result of the jet instabilities. The spatial scales of the unstable waves are somewhat larger at later stages in the calculation than those found on day 400. The time-averaged density flux (not shown) is positive between 825 and 1950 m with a maximum at 1187 m, in general agreement with that predicted by linear theory.

The three local maxima of the perturbation density flux in Figure 5b are associated with successive cycles of wave growth and zonal jet instabilities. It is important to note that the mesoscale eddies that result from instability of the early zonal jets do not interfere with the further growth of additional waves and the continued density flux due to baroclinic instability of the mean flow. As indicated in Figure 4, the flow in the nonlinear regime looks nothing like the large-scale flow used for initialization, yet the potential energy contained in the large-scale mean flow remains accessible to the baroclinic instability mechanism. It is the vertical shear of the large-scale flow, not the horizontal structure, which drives the instability. The third maximum at day 650 is relatively weak because the previous eddy fluxes have extracted essentially all of the potential energy from the mean state by this time. This finite amount of energy available to drive the unstable waves is a limitation of the periodic channel approximation of the model. In the real ocean the potential energy of the mean large-scale flow is continually replenished by additional forces that are not included in this simple model.

### 3.2. Salt Flux

The similarity between the middepth maximum in eddy density flux and the salinity anomaly of the Mediterranean salt tongue leads one to consider whether the salt carried by the unstable waves might be important in the overall salt balance in this region. The eddy salt flux may be related to the eddy density flux through the horizontal density ratio $R_H = \mathcal{A}\nabla\Theta/\mathcal{B}\nabla S$, where $\mathcal{A}$ and $\mathcal{B}$ are the thermal and haline expansion coefficients, $\Theta$ and $S$ are potential temperature and salinity, and $\nabla$ indicates the horizontal derivative. This ratio measures the relative influence of temperature and salinity on the horizontal gradient of density. If we assume that the local density anomaly is linearly related to the local potential temperature and salinity anomalies through the thermal and haline expansion coefficients, the eddy salt flux may be related to the eddy density flux as

$$uS' = \frac{u\rho'}{\mathcal{B}(1 - R_H)}. \tag{6}$$

The value of $R_H$ has been calculated from the climatological database of *Levitus* [1982]. Within the core of the salt tongue, $R_H$ is nearly uniform with depth and latitude and increases nearly linearly toward the west from 1.05 at 12°W near the outflow to 1.4 at 30°W. For $R_H > 1$ and $u\rho' > 0$ the net salt transport is to the west. This also corresponds to a net westward flux of heat at middepths, consistent with the offshore movement of the warm, salty Mediterranean water within the core of the tongue.

An estimate of the salt transported by the eddy fluxes is obtained by integrating the spatial and temporally averaged eddy density flux from the nonlinear model over the cross section of the Mediterranean salt tongue. This, of course, is a very idealized calculation considering the limitations of the model, however, it does demonstrate the order of magnitude of the salt that might be carried by these waves. Here we take a representative value of $\mathcal{B} = 0.77$ and estimate the cross-sectional area of the salt tongue to be $2 \times 10^9$ m$^2$, calculated from the Levitus climatology at 20°W where

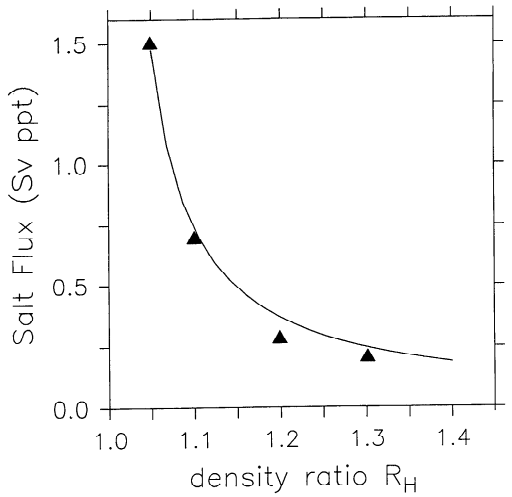


**Figure 6.** Zonal salt flux (Sv ppt $\approx 10^6$ kg s$^{-1}$) as a function of horizontal density ratio ($R_H = \mathcal{A}\nabla\Theta/\mathcal{B}\nabla S$), symbols are for model calculations with temperature and salinity; the solid line is from the model with density only (making use of relation (3)).

the local salinity exceeds the background salinity by an amount greater than 0.05 ppt between the potential temperature surfaces 3.5°C and 12.0°C. The zonal density flux is calculated from the meridional and temporal average of the model eddy density flux at the center of the channel (longitude = 200 km). The total salt flux $\mathcal{S}$ is then obtained by making use of relation (6) as

$$\mathcal{S} = \int_A \frac{\overline{u\rho'}^{yt}}{\mathcal{B}(1 - R_H)} dA. \tag{7}$$

where $\overline{u\rho'}^{yt}$ is the meridional and temporal average of the model zonal density flux and $A$ is the cross-sectional area of the salt tongue. The total westward salt flux as a function of the horizontal density ratio is given by the curve in Figure 6. As indicated by (7), the salt flux becomes very large as $R_H \to 1$. However, for density ratios representative of the core of the salt tongue, the total westward salt flux is between 1.5 Sv ppt and 0.2 Sv ppt and is not very sensitive to further increases in $R_H$ (1 Sv ppt = $10^6$ m$^3$ s$^{-1}$ ppt $\approx 10^6$ kg s$^{-1}$). The zonal salt flux was also calculated from four model calculations that used temperature and salinity together with a linear equation of state instead of density only. As indicated by the symbols in Figure 6, the magnitude of the total salt flux, and its dependence on $R_H$ is reproduced well by these independent calculations. This result demonstrates that relation (6) is valid and that the total salt flux is controlled by the density field, not the salinity field (except through the value of $R_H$). (Because of the computational expense, these calculations were done at slightly lower resolution, 10 km horizontal and 15 modes in the vertical; however, the behavior is qualitatively similar to the higher-resolution calculation, which used density only.)

The total anomalous salt flux through the Strait of Gibraltar is estimated by *Bryden and Kinder* [1991] to be 1.61 Sv ppt. Considering that 25% of the total flux may be carried by Meddies [*Richardson et al.*, 1989], this leaves 1.20 Sv ppt to be carried by the traditional advective/diffusive balance. Therefore the density fluxes driven by the present simple baroclinic instability mechanism could result in a significant amount of the total estimated salt flux within the salt tongue.

## 4. Relation to Observations and Large-Scale Models

Direct evidence of salt transport by such zonal jets in the Mediterranean salt tongue is difficult to obtain from observations. There is, however, some indication that zonal jets with large salinity anomalies are present in the hydrographic sections described by *Richardson et al.* [1991]. A meridional section at 20°W indicates that the core of the salt tongue north of 35°N is not simply a large-scale feature with gradually varying salinity, but rather it is made up of many smaller features with meridional scales on the order of the data resolution (50–100 km), and vertical scales of the order of 1000 m. The traditional interpretation of such variability is that it is due to mesoscale eddies and Meddies, however, if that were the case one would expect similar scales of variability in the zonal direction. A zonal section along 36°N reveals much less small scale variability within the core of the salt tongue, supporting instead the interpretation that the small scales in the meridional section are the signature of the zonal jets, consistent with the proposed baroclinic instability mechanism.

The variability predicted by the present theory would also explain the existence of local salinity anomalies found in climatological hydrographic data by *Richardson et al.* [1991]. They found 36 observations with salinity anomalies between 0.3 and 0.4 ppt in the region bounded by 25°W and the coast and 30°N and 47°N with most north of 35°N. This is coincident with the region where the baroclinic instability mechanism is expected to be most effective. In fact, *Richardson et al.* [1991] believed that these anomalies were not due to weak Meddies but rather the result of time-dependent velocity fluctuations carrying salty water across mean isohalines. In addition, C. Maillard (private communication, 1992) found an almost equivalent number of equal strength negative anomalies in this same region. This would argue against their being due to weak or decaying Meddies or westward jets of Mediterranean water, which would have positive anomalies only, and consistent with the perturbations that would be induced by both eastward and westward flowing zonal jets as a result of the unstable waves.

Similar variability was found in the Mediterranean salt tongue of a basin scale eddy resolving primitive equation model (community modeling effort model) by

*Spall* [1990]. These currents were nearly zonal, persisted for 1–2 years, had strengths of approximately 2 $cm^2\ s^{-1}$, southward phase speeds of 0.2 $cm^2\ s^{-1}$, and had a strong signature in the salinity field. The meridional scale of the jets was approximately 200 km, somewhat larger than that predicted by the present linear stability analysis but perhaps limited by the horizontal resolution of the model, which was approximately 35 km at these latitudes. Furthermore, the zonal eddy density flux was found to be weakly negative in the upper 500 m north of 20°N, consistent with the present baroclinic instability theory. Similar low-frequency, zonal wave motions are also observed in the eastern basin of a model of the North Pacific (H. E. Hurlburt, private communication, 1992). The apparent existence of the baroclinic instability mechanism in such complex models is important because it suggests that the basic theory presented here may be robust in the presence of surface wind and buoyancy forcing, mesoscale eddies, strong frontal regions, bottom topography, and long time integrations.

## 5. Conclusions

A theory for the source of low-frequency variability in the interior of ocean subtropical gyres and its role in the zonal flux of density (or temperature and salinity) is discussed with specific application to the Mediterranean salt tongue region. The two main points are (1) baroclinic instability of large-scale flows typical of subtropical gyre interiors results in low-frequency zonal motions and (2) the associated eddy fluxes may carry an appreciable amount of salt and heat to the west within the core of the Mediterranean salt tongue.

The present zonal salt flux is achieved by low-frequency variability, but it is not directly related to the mean salinity field, as many parameterizations of mixing due to eddies in large scale models assume. Any parameterization of the present mechanism for zonal salt flux must be dependent on the mean zonal density gradient (the energy source for the waves) and the horizontal density ratio (which relates density flux to salt flux). An effective parameterization must also reflect the enhanced transport in the zonal direction that results from the stabilizing effect of the planetary vorticity gradient, as opposed to the eddy flux being down the largest mean density or salinity gradient. This is a fundamentally different mechanism from traditional mixing due to mesoscale eddies and, as such, its importance in the overall salt balance may not be accurately reflected by the relatively low values of eddy kinetic energy in the low-frequency band. The presence of such energetic low-frequency motions implies that if one is to estimate the mean flow from time series of observations that periods of the order of 3 to 10 years must be resolved.

Several complicating features of the real ocean have been neglected in the present analysis in order to obtain a clear and understandable treatment of the instability mechanism. It would be interesting to investigate this mechanism in the context of a more complete ocean model which includes fronts, Meddies, mesoscale eddies from other sources, surface forcing, an explicit Mediterranean outflow, and fine scale mixing. The results presented here provide an understanding to the underlying dynamics, and the key features with which to test these simple ideas in both observations and more complex models.

**Acknowledgments.** The bulk of this work was supported by NSF grant OCE–9009463 while M.A.S. was at the Woods Hole Oceanographic Institution. Final analysis and revisions were completed at the Institut für Meereskunde in Kiel, Germany, under the support of the Bundesminister für Forschung und Technologie grant 03F0050D. I would like to thank Joe Pedlosky for suggesting baroclinic instability of the nonzonal flow as a means of generating zonal low-frequency variability. Many of the calculations presented in this paper were carried out on the Cray YMP at the National Center for Atmospheric Research, which is sponsored by the National Science Foundation. This paper is contribution number 8049 of the Woods Hole Oceanographic Institution.

## References

Arhan, M., On the large scale dynamics of the Mediterranean outflow, *Deep Sea Res., 34,* 1187–1208, 1987.

Bryden, H. L., and T. H. Kinder, Steady two-layer exchange through the Strait of Gibraltar, *Deep Sea Res., 38,* S445–S463, 1991.

Haidvogel, D. B., J. L. Wilkin, and R. Young, A semi-spectral primitive equation ocean circulation model using vertical sigma coordinates and orthogonal curvilinear horizontal coordinates, *J. Comp. Phys., 94,* 151–185, 1991.

Hogg, N. G., A least-squares fit of the advective–diffusive equations to the Levitus Atlas data, *J. Mar. Res., 45,* 347–375, 1987.

Levitus, S., Climatological atlas of the world ocean, *NOAA Prof. Pap., 13,* 173 pp., 1982.

Maillard, C., Atlas hydrologique de l'Atlantic Nort-Est, *Inst. Fr. Rech. Exploit. Mer Brest,* 32 pp., 1986.

Müller, T. J., and G. Siedler, Multi-year current time series in the eastern North Atlantic Ocean, *J. Mar. Res., 50,* 63–98, 1992.

Pedlosky, J., On the stability of currents in the atmosphere and the ocean, Part 1, *J. Atmos. Sci., 21,* 201–219, 1964.

Pedlosky, J., *Geophysical Fluid Dynamics,* 624 pp., Springer-Verlag, New York, 1979.

Richardson, P. L., and K. Mooney, The Mediterranean outflow — A simple advection–diffusion model, *J. Phys. Oceanogr., 5,* 476–482, 1975.

Richardson, P. L., D. Walsh, L. Armi, M. Schröder, and J. F. Price, Tracking three Meddies with SOFAR floats, *J. Phys. Ocean., 19,* 371–383, 1989.

Richardson, P. L., M. S. McCartney, and C. Maillard, A search for meddies in historical data, *Dyn. Atmos. Oceans, 15,* 241–265, 1991.

Saunders, P. M., Circulation in the eastern North Atlantic, *J. Mar. Res., 40,* 641–657, 1982.

Schmitz, W. J., J. F. Price, and P. L. Richardson, Recent moored current meter and SOFAR float observations in the eastern Atlantic near 32N, *J. Mar. Res., 46*, 301–319, 1988.

Schopp, R., and M. Arhan, A ventilated middepth circulation model for the eastern North Atlantic, *J. Phys. Oceanogr., 16,* 344–357, 1986.

Spall, M. A., Circulation in the Canary Basin: A model/data analysis, *J. Geophys. Res., 95*, 9611–9628, 1990.

Spall, M. A., P. L. Richardson, and J. F. Price, Advection and eddy mixing in the Mediterranean salt tongue, *J. Mar. Res., 51*, 797–818, 1993.

Tziperman, E., The Mediterranean outflow as an example of a deep buoyancy-driven flow, *J. Geophys. Res., 92*, 14,510–14,520, 1987.

---

M. A. Spall, Woods Hole Oceanographic Institution, Woods Hole, MA 02543. (e-mail: spall@cms.whoi.edu)

(Received September 7, 1993; December 3, 1993; accepted December 7, 1993.)